

On using surface-source downhole-receiver logging to determine seismic slownesses

David M. Boore^{a,*}, Eric M. Thompson^b

^a*U.S. Geological Survey, 345 Middlefield Road, Menlo Park, CA 94025, USA*

^b*Department of Civil and Environmental Engineering, Tufts University, 113 Anderson Hall, Medford, MA 02155, USA*

Received 11 November 2006; accepted 15 March 2007

Abstract

We present a method to solve for slowness models from surface-source downhole-receiver seismic travel-times. The method estimates the slownesses in a single inversion of the travel-times from all receiver depths and accounts for refractions at layer boundaries. The number and location of layer interfaces in the model can be selected based on lithologic changes or linear trends in the travel-time data. The interfaces based on linear trends in the data can be picked manually or by an automated algorithm. We illustrate the method with example sites for which geologic descriptions of the subsurface materials and independent slowness measurements are available. At each site we present slowness models that result from different interpretations of the data. The examples were carefully selected to address the reliability of interface-selection and the ability of the inversion to identify thin layers, large slowness contrasts, and slowness gradients. Additionally, we compare the models in terms of ground-motion amplification. These plots illustrate the sensitivity of site amplifications to the uncertainties in the slowness model. We show that one-dimensional site amplifications are insensitive to thin layers in the slowness models; although slowness is variable over short ranges of depth, this variability has little effect on ground-motion amplification at frequencies up to 5 Hz.

Published by Elsevier Ltd.

Keywords: Site-response; Shear-wave velocity; Ground motion amplification

1. Introduction

The material properties at relatively shallow depths are useful to anyone studying earthquake ground motions at the Earth's surface. Seismologists seeking information about the source or the parts of the travel path between the source and the near-surface need to remove the response of these local materials, often called site effects. On the other hand, engineers need to know how the amplitude, frequency content, and duration of the ground motion will be changed by the near-surface material properties of the ground for seismic hazard assessment and to predict the ground motions that are likely to occur at a site. Both theoretical and empirical studies have confirmed that the near-surface shear-wave slowness (or its reciprocal, shear-wave velocity) is a controlling factor of

the ground motion that is observed at a specific site [1–3]. In this paper we discuss interpretations of slowness surveys as related to site effects, also called site amplification or site-response. Although noninvasive methods for imaging slowness are becoming more important [4], invasive methods give direct information about the subsurface. Boore [5] briefly describes the methods used by a group at the USGS for interpreting surface-source downhole seismic measurements, and here we present a more thorough discussion. The method applies equally well to measurements made in boreholes and from seismic cone penetration tests (SCPT).

Various uses of near-surface seismic slownesses require different measurement/interpretation methods. For example, correlations of shear-wave slowness within geologic units (e.g., Refs. [6–8]) do not require a model extending to the surface and slownesses calculated for the intervals between travel-time measurements may be sufficient. Alternatively, site-amplification calculations require

*Corresponding author.

E-mail address: boore@usgs.gov (D.M. Boore).

a continuous model extending from the surface, but details of thin layers are usually not important. The shear-wave slowness of thin layers may be important, however, for other applications such as determining the critical layer in liquefaction studies (e.g., Refs. [9,10]). Our emphasis in this paper is on developing models of the slowness extending from the surface to depth, for the purpose of site-amplification studies.

The paper with the most similar content to ours is Kim et al. [11], which discusses the accuracy and limitations of several methods for obtaining slowness profiles from downhole seismic data. Our paper differs in a number of important aspects from theirs. The method we present is most similar to the method that Kim et al. [11] call the Snell's Law Ray-Path Method, but our method allows for any number of arbitrarily located layer interfaces, whereas Kim et al. [11] assume that layer interfaces are located at the depths of travel-time measurements. In addition, given the layer interfaces, the Kim et al. [11] method builds the model stepwise, one layer at a time, while the method we employ solves for the slowness in each layer by minimizing the mean squared difference between the observed and predicted travel-times over all receiver depths, accounting for refraction at layer boundaries. We present comparisons of models obtained by different methods from the same travel-time data, similar to the comparisons in Kim et al. [11], but we further compare the difference in site amplifications that result from the differences in these profiles. While Kim et al. [11] briefly discuss how layer boundaries can be inferred from the travel-time data, we emphasize the importance and subjectivity of the number and location of the interfaces in a slowness model.

This paper only considers models comprising stacks of constant slowness layers. Wave propagation predicts that travel-time data should be composed of essentially linear segments for such models. The majority of the travel-time data that we have analyzed exhibit these linear segments, suggesting that the structure beneath a site can be accurately represented by a stack of constant slowness layers. Consistent with this finding, Holzer et al. [6] found no depth dependence of slowness within near-surface sedimentary geologic units. In cases where the slowness of a geologic unit is better represented by a gradient, however, a representation of the structure by a stack of constant slowness layers is sufficient for site-response analysis.

The key variable in these interpretations are the depths to interfaces, or the "depth-to-bottom" of each layer. Automatic picking of layer boundaries is possible because a change in the slope in the travel-time plot indicates the location of an interface. We discuss the use and limitations of an algorithm for automatic detection of interfaces presented by Thompson [12]. After describing the imaging method (which applies both for manual and automatic picking of the interface depths), we illustrate it with a series of examples from borehole sites for which geologic descriptions of the materials, as well as independent

slowness measurements, are available. The sites chosen represent a spectrum of possible slowness vs. depth profiles. All examples are for S-wave slowness, although the same methods work equally well for P-wave slowness.

We start with a review of the interpretation of surface-source downhole-receiver (SSDHR) logging using manually determined depths to interfaces. This is followed by a discussion of an algorithm that picks the interface depths automatically. We then apply the methods to a series of sites that illustrate some of the difficulties that can be encountered. Finally, we discuss the sensitivity of the site amplifications to uncertainties in the derived slowness profiles.

2. Comparing models

Comparisons of models in this paper are in terms of slowness (inverse velocity, with units of s/km) rather than velocity. As discussed in Brown et al. [13] there are a number of advantages to this convention. First, it is a more fundamental parameter for site-response studies in that the travel-time across layered structures is linearly proportional to the slowness ($t = s \times h$, where t is travel-time, s is slowness, and h is layer thickness). Thus, it is more direct to speak in terms of slowness rather than its reciprocal, velocity. Second, slowness can be linearly averaged to get depth-averaged values, whereas it is incorrect to linearly average velocity to get, for example, the average velocity of the upper 30 m, $V_s(30)$. Third, statistical properties associated with fitting the travel-time data, such as the standard errors, apply to slowness rather than velocity. Fourth, comparing slowness profiles is more appropriate for site-response analysis because it emphasizes the properties of the materials that amplify ground motions rather than the stiffer materials that are less important for site-response. Fig. 1 compares two models of subsurface slowness and velocity obtained at the Garner Valley downhole array site in California. The velocity plot is dominated by the large difference in velocity at depths beyond 60 m, whereas the slowness plot minimizes this difference, concentrating instead on the material properties closer to the surface. Although the profiles for the two models are not identical, in terms of slowness they are similar.

Another way of comparing profiles is in terms of the site amplification predicted for the profiles. Such comparisons are useful because they address the question of whether differences between slowness models are of practical consequence. There are a variety of ways to compute the site amplification for a given slowness profile. Boore and Brown [14,15] and Brown et al. [13] advocate using the ratio of simplified amplifications based on the seismic impedance changes in the models. These amplifications do not have resonant peaks and troughs, and therefore the ratios are not dominated by slight differences in the frequencies at which the peaks and troughs occur. In this paper, however, we compare site amplifications using the

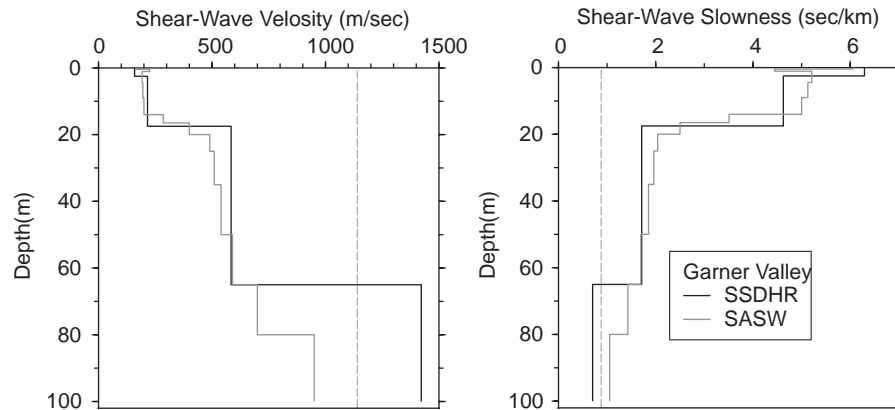


Fig. 1. Comparison of models using plots of velocity and slowness vs. depth. The dashed gray line shows the halfspace velocity and slowness used in the site-response calculations. (Surface-source downhole-receiver (SSDHR) model from Boore [5]; SASW model from Brown et al. [13]).

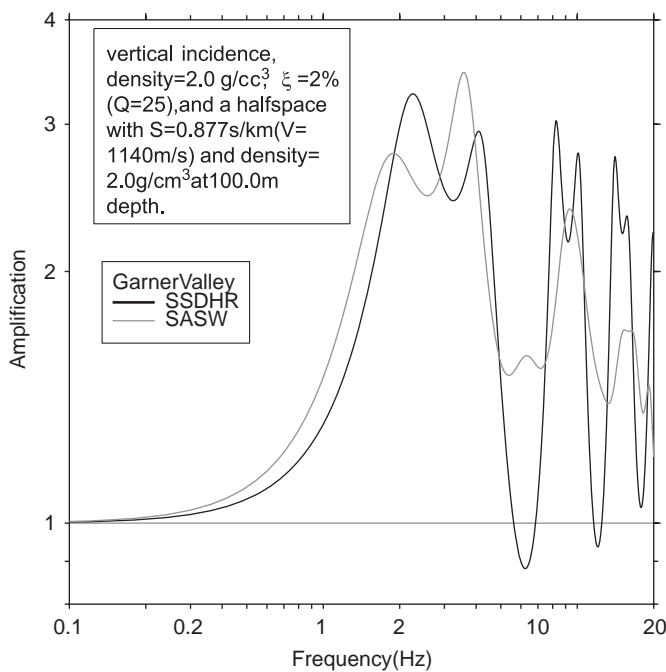


Fig. 2. Amplifications for the two models at Garner Valley shown in Fig. 1. Information about the amplifications, including the reference condition, is given in the figure.

horizontal component of S-waves (SH-waves) assuming one-dimensional vertically incident propagation, with all reverberations included. We do this because many of the models that we will be comparing are not that dissimilar from one another. Calculations of site amplification using one-dimensional vertically incident SH-waves often gives only a general approximation of the actual site amplification (e.g., Refs. [3,4]). For this reason, we use the plots of amplification only as a general comparison of profiles; it would be a mistake to attribute much meaning to differences in the details of the amplifications, particularly at higher frequencies, and certainly plotting ratios of the amplifications must be avoided. In Fig. 2, we show

amplifications for the slowness models from Fig. 1. Although there are clear differences, due to the variability between the models, particularly at shallow depths, overall the amplifications are quite similar.

3. Imaging slowness as a function of depth

3.1. Inversion of travel-times

This paper is concerned with the inversion of travel-times from a surface-source to a series of depths beneath the surface. These travel-times can be obtained in a number of ways, from measurements made in boreholes to those made using SCPT surveys (e.g., Ref. [4]). The travel-times can be based on manually picked first arrivals of the direct S-wave (and all of the travel-times analyzed in this paper were determined in this way) or using cross-correlation of traces (e.g., Ref. [16]), as long as the times represent the travel-time of the wave from the surface rather than a difference in travel-time between two depths. This requirement is necessary because we derive models of slowness from the surface to depth, not just interval-slownesses (the slowness calculated between two adjacent sampled depths, as is commonly practiced). It is not in the scope of this paper to discuss the advantages and disadvantages of different methods for obtaining the travel-times. The researcher responsible for picking the travel-times should record the precision of the picks, which can be substantially different within the same borehole. We use a convention of estimating the standard deviation of each travel-time measurement normalized to the standard deviation of the best pick in a profile (approximately 1 ms). Travel-time curves presented in this paper indicate this relative value by the color of the point corresponding to each measurement, as indicated in each figure showing travel-times.

Interpretations of these data are often based on corrections of the observed travel-time to equivalent vertical travel-time, as if the source were not offset, using

the equation

$$tt^{vrt} = tt^{obs} \frac{z}{\sqrt{h^2 + z^2}},$$

where h is the horizontal offset of the source from the borehole, tt^{obs} is the measured travel-time from the surface-source to depth z and tt^{vrt} is an approximation of the equivalent vertically incident travel-time, which assumes that the ray-paths of the recorded waves are straight lines, with no refraction at layer boundaries. (Liu et al. [17] show from Fermat's principle of least time that interval-slownesses obtained using tt^{vrt} are usually close to the actual slownesses.) Fig. 3 shows tt^{obs} and tt^{vrt} as a function of depth for one of the sites discussed at length in this paper. Fig. 3 also shows that the trend in the corrected-to-vertical data should go through the origin, whereas the observed data is offset (theoretically at $h \times s_1$, where s_1 is the slowness of the surface layer) at zero depth. The inversion of either tt^{obs} or tt^{vrt} is based on solving for slowness in a stack of layers, within each of which the slowness is assumed to be constant (see Fig. 4 for geometry and notation). For a given set of interface depths, an inversion computes the slownesses in each layer such that the square of the differences in the observed and predicted travel-times, summed over all observations, is minimized. The inversion is linear in terms of the slowness in each layer (e.g., Ref. [18]). The measurements are inversely weighted by the estimated relative standard deviation of each travel-time pick. When the travel-times have been corrected to an effective vertical source using the equation above (or equivalently, when non-corrected travel-times are used

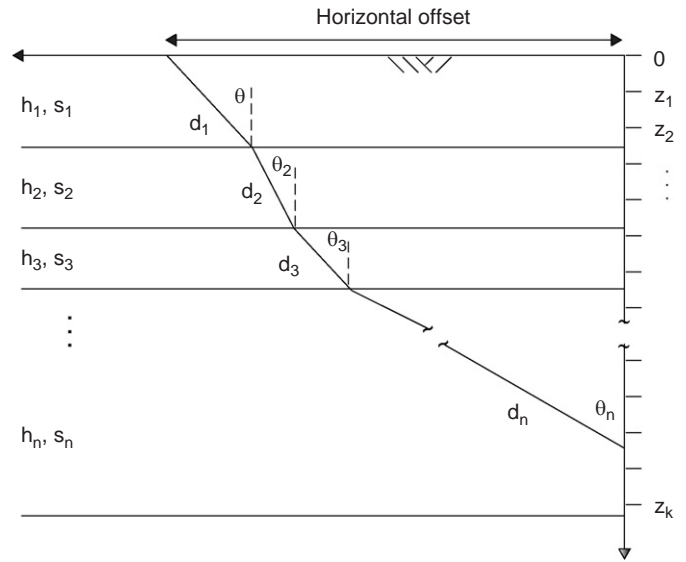


Fig. 4. Ray diagram illustrating the variables in the inversion. The model of n -horizontal layers has thickness $h = (h_1, \dots, h_n)^T$, and slowness $s = (s_1, \dots, s_n)^T$. The ray travels a distance $d = (d_1, \dots, d_n)^T$ in each layer with an angle of incidence $\theta = (\theta_1, \dots, \theta_n)^T$. The k -travel-time measurements $tt = (tt_1, \dots, tt_k)^T$ are measured at depths $z = (z_1, \dots, z_n)^T$ in the borehole.

with the assumption that the path between source and recorder is not refracted at interfaces), this procedure fits all observed travel-times in a least-squares sense in a single weighted linear inversion. Iteration is required, however, to generalize the inversion to account for refraction at interfaces. The initial set of slownesses for each layer is computed assuming non-refracted ray-paths. Given this set of initial layer slownesses, we solve the two-point boundary-value problem to find the take-off angles for the rays traveling from the source to each depth; these angles are used to compute the distance traveled in each layer, and then a new set of slownesses is determined. The model is updated in this fashion until the maximum difference between consecutive sets of layer slownesses is acceptably small. See Thompson [12] for complete details of the inversion and codes that implement these methods in the statistical language and environment R [19].

3.2. Manual determination of interface depths

The most difficult and subjective task in obtaining a model from a set of travel-times is determining a set of depths to the interfaces between layers. This is true whether or not refraction of ray-paths is assumed. We discuss several ways of determining these depths.

In most cases, some indication of subsurface lithology will be available (from drill cuttings, the drilling rate, or the penetration resistance of a SCPT probe). The initial set of interface depths for the inversion can be set to the depths of distinct changes in lithology. For example, Fig. 5 shows the geological and lithological information available for the Jensen Main Building (JMB) site in California [20]; the set of records from which the travel-times were determined is

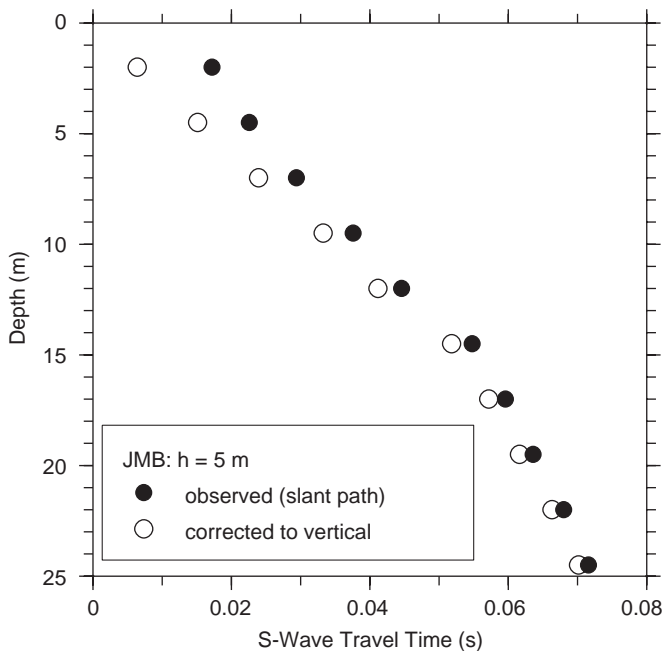


Fig. 3. Observed and corrected-to-vertical travel-times at Jensen Main Building (JMB). The horizontal offset from the source to the borehole is 5 m (travel-times from Gibbs et al. [20]).

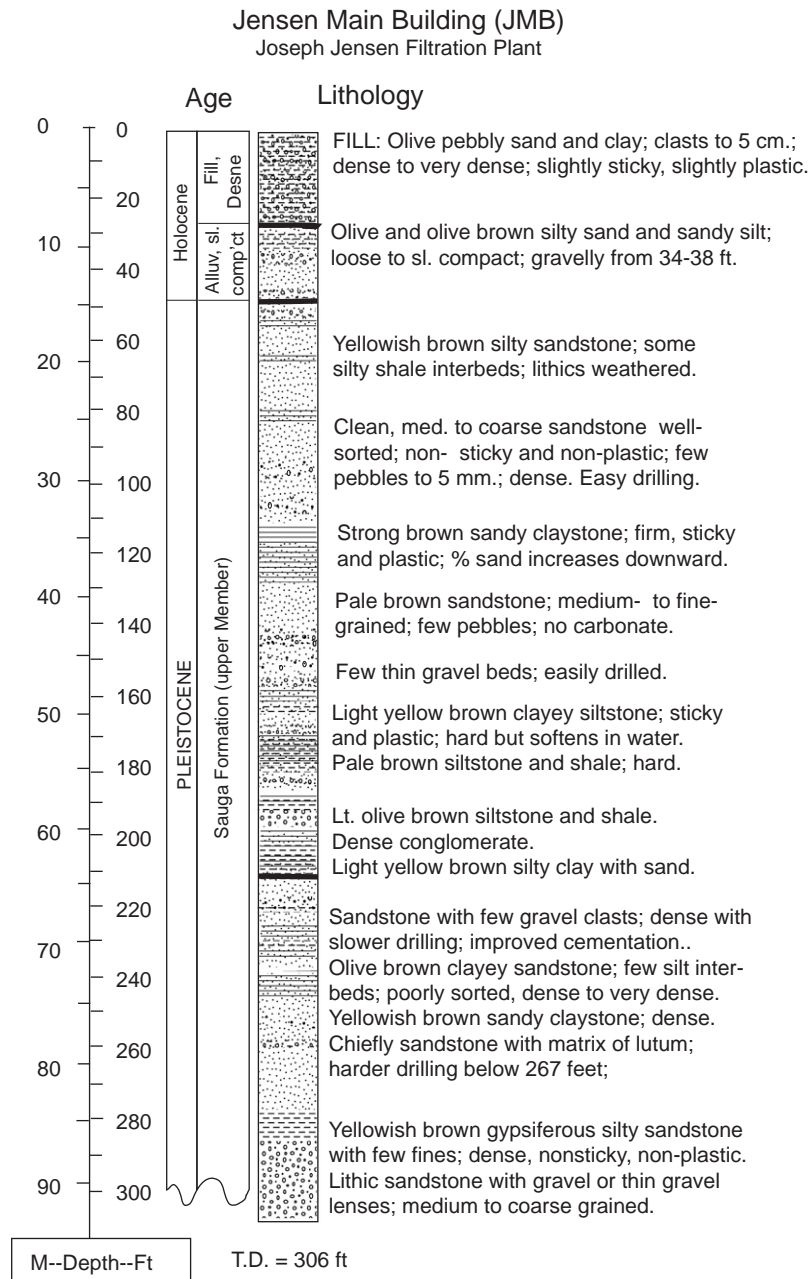


Fig. 5. Geologic information at the Jensen Main Building site (adapted from Gibbs et al. [20]). A geologist describes and records the lithology that is encountered as the borehole is drilled.

shown in Fig. 6. The surface layer is approximately 9 m of fill, which is underlain by 6 m of compact and gravelly Holocene material resting on Pleistocene sandstone. The geologic description also indicates a change in the type of sandstone at a depth of 63 m. Fig. 7 shows the model that results from the inversion with the set of interface depths based on these lithologic changes. This figure shows the travel-times, the residuals between the observed and predicted travel-times (accounting for refraction at layer boundaries), and the slowness model. Note that the Holocene–Pleistocene boundary corresponds to a distinct change in slope of the travel-times vs. depth curve.

The residuals in Fig. 7 display linear trends with depth, implying that further layering is required in the model. In practice at the U.S. Geological Survey, where borehole data have been recorded and analyzed for more than 30 years, the interpretation is often a collaboration between the seismologist who picked the first-arrival times from the records and the geologist who observed and described the cuttings that came to the surface as the borehole was drilled (e.g., Ref. [5]). The lithology-based set of interface depths provides the starting model, with subsequent refinement as needed to better match the travel-times (as long as the layering does not result in a major violation of the geologic

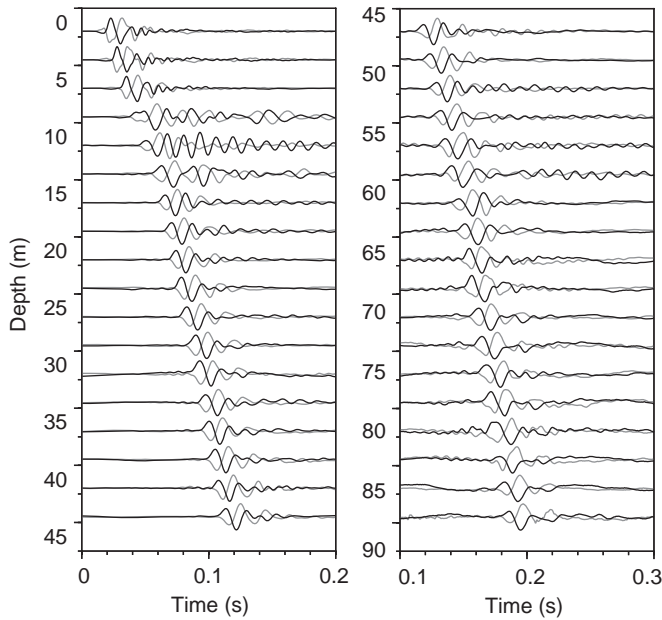


Fig. 6. Time series at the Jensen Main Building site from the surface source, recorded at various depths. The source is activated in directions 180° apart, resulting in two sets of time series with opposite polarity (as indicated by the black and gray lines). Note that the time scale for the right-hand panel of graphs starts at 0.1 s, not 0.0 s as in the left-hand panel (adapted from Gibbs et al. [20]).

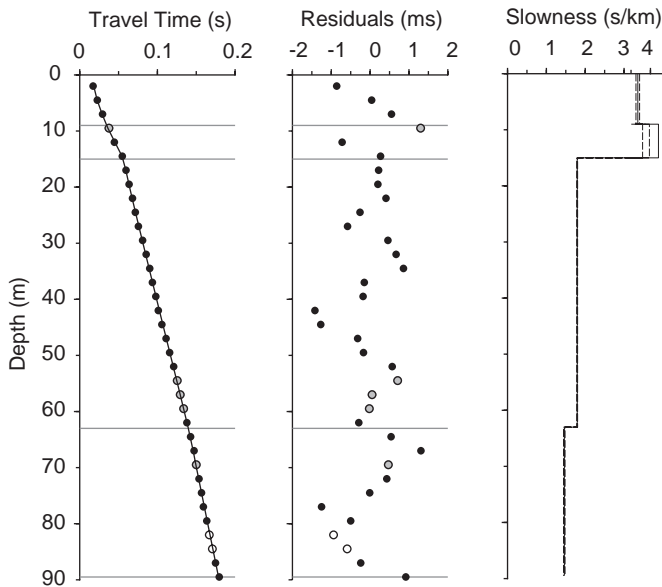


Fig. 7. Travel-times, residuals, and slowness for a model based solely on the lithology at the Jensen Main Building site (JMB). The symbols indicate the uncertainty of the travel-times, as multiplicative factors relative to the uncertainty of the points shown in black (gray = 2; open = 3).

interpretation and geophysical logs obtained in the borehole). Geologic logs are not always available, and furthermore, changes in lithology do not always provide a complete determination of layer interfaces. In these cases the interface depths can be determined solely from the

travel-times (and often the differences between the models determined from the seismologist–geologist collaboration and from the lithology-blind interpretation are minor). We implement this manual procedure in an iterative fashion. The procedure begins with a homogeneous model and iteratively adds interfaces until the residuals appear to be randomly distributed with respect to depth. While iteratively searching for patterns in residuals is often given the derogatory term, “data dredging,” we think there is merit in using the residuals for model selection in this specific application. The physics of wave propagation predicts that a model consisting of a stack of constant slowness layers will produce essentially linear segments in the travel-time measurements. The slopes of these segments are equal to the slownesses of the respective layers (at depths far enough from the surface to be on the limb of the hyperbolic travel-time curve when using times not corrected to tt^{vrt}). Therefore, changes in the slope indicate a change in slowness, and the presence of linear trends in the residuals of a model indicate that one or more unidentified interface exists. Such trends can occur, however, as the result of biases in picking travel-times, as the picks are often guided by trends in arrivals on nearby records; poor records at one depth might cause a time to be picked early or late, and the times at better recorded nearby depths might be unintentionally adjusted by the analyst to yield continuity of the arrivals. Our imaging method allows for unequal weights of travel-times as one way of diminishing the impact of poorly recorded data. As we will show in the examples presented later, gradients in slowness can be approximated by a series of constant slowness layers, and again the trends in the residuals are used to establish a set of interface depths.

Fig. 8 illustrates the process of building a model at the JMB site in southern California [20] by iteratively adding interfaces (and thus layers) until the residuals do not contain linear trends. Each row of plots summarizes a step of the process. The first column of plots shows the observed travel-time data as points; the line connects the predicted values for the model at each depth. The second column of plots is the distribution of the residuals with depth for each iterative step. The third column of plots is the slowness profile for each iteration, and the dotted lines show the slowness plus and minus one standard deviation. The first row is the single layer model, and clearly does a poor job predicting the measured travel-time data. The most obvious change in slope of the residuals in the single layer model is at approximately 15 m (this depth corresponds to a major change in lithology from sand and silt to sandstone, as shown in Fig. 5). The second model contains an additional interface at this depth, but there are still clear linear trends in the residuals. The third model contains an additional interface at approximately 65 m, as suggested by the change in slope of the residuals at this depth in the second model (this depth also corresponds to a change in lithology). The fourth model is the final model in the process and contains 11 layers. The residuals do not

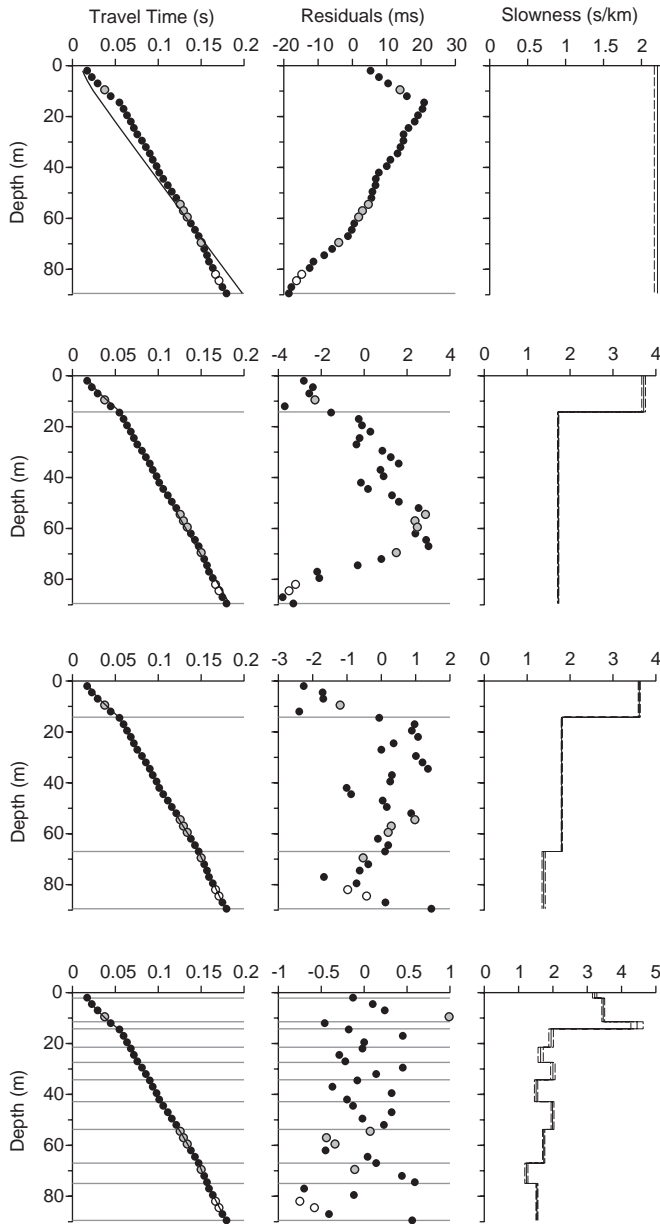


Fig. 8. A sequence of models for the Jensen Main Building site. Subsequent models have additional layer interfaces. Each row of plots summarizes a step of the process. The first column of plots shows the observed travel-time data (symbols) and the predicted model (line). The second column of plots is the distribution of the residuals with depth for each step. The third column of plots is the slowness profile at each step and the dotted lines show the slowness plus and minus one standard deviation. The symbols indicate the uncertainty of the travel-times, as multiplicative factors relative to the uncertainty of the points shown in black (gray = 2; open = 3).

contain the strong linear trends that are present in the residuals of the model based solely on lithology (Fig. 7).

3.3. Automatic determination of interface depths

Although the imaging method described in the previous section works well, it is subjective and can be time consuming when analyzing data from many sites. For this

reason it is useful to develop an automatic procedure for determining interface depths. Such a method can be used by itself or to provide a starting model that can be refined with manual picking of the interface depths. We have developed automatic routines that attempt to reproduce the steps, described in the previous section, of manually building a model based on the travel-time data. While a near-perfect fit to the observations can be obtained when the number of interfaces in the model approaches the number of observed travel-times, we attempt to find a parsimonious model by only accepting new interfaces if the bias-adjusted Akaike’s Information Criterion [21–23], AIC_c , of the model with the additional interface is less than the model without the additional interface. AIC_c is a relative measurement of badness-of-fit for comparing different models. It is a function of not only the model variance, given by the maximum likelihood estimator $\hat{\sigma}^2 = RSS/k$, but also the number of observations, k , and the number of estimated regression parameters $N = n + 1$ (number of interfaces, n , plus one for σ^2), as given by

$$AIC_c = k \log(\hat{\sigma}^2) + \frac{2NK}{k - N - 1},$$

and the residual sum of squares is given by

$$RSS = \sum_{i=1}^k (tt_i^{obs} - tt_i^{pred})^2.$$

In this equation, tt^{obs} are the observed travel-time measurements, tt^{pred} are the corresponding predicted travel-time measurements. Our algorithm consists of the following iterative steps:

1. Using a previous set of interface depths, Z (the first set is simply a single layer with thickness equal to the depth to the deepest measurement), compute the weighted RSS for each layer (termed WRSSL, which is the residual sum of squares weighted by the number of travel-time measurements in each layer).
2. Choose the layer with the largest WRSSL.
3. Within this layer, find the depth of an additional interface that minimizes the RSS of the entire model. Compute the AIC_c for the new set of interfaces. If the AIC_c decreases, add the layer and start again at step 1. If the AIC_c increases, then do not add an interface, but move to the layer with the next largest WRSSL and repeat this step. The algorithm ends when no new interfaces can be added without increasing AIC_c .

The travel-times, residuals, and slowness for the JMB site are shown in Fig. 9, using the automatic algorithm to determine the set of interface depths. There are more layers than in the lithology-based model (Fig. 7), but fewer than in the model based in manual fitting of the travel-times (Fig. 8). Most of the clear trends in the residuals seen in Fig. 7 have been eliminated.

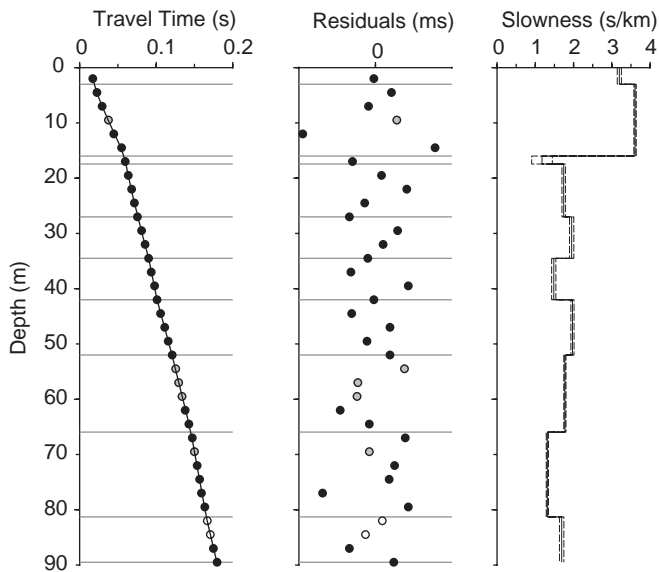


Fig. 9. Travel-times, residuals, and slowness for model with depth-to-interfaces picked automatically (JMB site). The symbols indicate the uncertainty of the travel-times, as multiplicative factors relative to the uncertainty of the points shown in black (gray = 2; open = 3).

4. Selected examples

In this section we show examples from a number of sites to illustrate how the methods handle various types of slowness profiles. We consider examples to illustrate surface-source downhole-receiver surveys with travel-time errors that increase with depth, sites with gradients in slowness rather than discrete interfaces, sites with thin layers, and sites with strong contrasts in slowness across an interface. For all cases we show amplifications for the set of models. The amplifications are from the program NRAT-TLE, written by Mueller [24] with modification by Herrmann [25], included in the SMSIM set of Fortran programs for simulating ground motions [26]. The program includes all reverberations within the stack of layers, for plane SH-waves incident from within a uniform-slowness halfspace at a specified angle. For all amplifications shown here we use vertical incidence, and for the halfspace we use a slowness close to that at the bottom of the site (to avoid the resonances associated with an arbitrary large impedance contrast between the bottom of the SSDHR models and the assumed halfspace).

For each site we show the slowness models using a number of sets of interface depths: those determined from the automatic algorithm, those from previously published models (if available), and those from manual fitting of the travel-times (often we show several such models, with increasing number of layers).

If available, we also plot the slownesses obtained from suspension logging; this method makes use of a probe lowered into a hole, on which a source near the bottom of the probe emits acoustic waves which are coupled into P- and S-waves at the edges of the borehole [27–29]. These

waves travel in the surrounding material and are reconverted into acoustic waves, which are then recorded on two receivers mounted 1 m apart (the first receiver is 2.1 m from the source). The wave slownesses are given by the difference in travel-times at the two receivers. Potentially the suspension logging results have higher resolution than SSDHR surveys because the waves have center frequencies near 1000 Hz, whereas those from the SSDHR surveys have dominant frequencies near 50 Hz.

We use the slowness measured by suspension logging as an independent measurement to compare the SSDHR slowness models against. It is important to note that the SSDHR models were developed “blind” with respect to the suspension log data. The suspension logging is also more capable of identifying thin layers because both the source and receiver are in situ, and so the measurement is not influenced by the effects of overlying sediments, as in the SSDHR surveys. More importantly, the sampling interval of the suspension logging is typically spaced at 0.5 or 1 m intervals, while the SSDHR surveys that we analyze have sampling intervals from 2 to 5 m. Some researchers may view the large amount of scatter that is present in much of the suspension logging as “noise” or error in the measurement; Wentworth and Tinsley [30], however, showed that these fluctuations can be well correlated with lithologic changes, which indicates that these fluctuations likely represent the true slowness fluctuations of the material adjacent to the borehole.

4.1. A typical site (JMB)

The downhole seismic data and the resulting models at site JMB are typical of many of the sites that we have analyzed. We use a series of models at this site that illustrate the variability in the slowness profiles that can result from selecting layer interfaces by different methods. Fig. 10 shows the slowness profiles for these models. The lithology (see Fig. 5) and travel-times indicate a sharp change in slowness across the Holocene–Pleistocene interface at 15 m. This change is found in all the SSDHR models, although it is interesting that the suspension-log model shows a gradient between about 15 and 22 m. The SSDHR travel-times do not seem to be consistent with this, although the 2.5 m spacing of the travel-times may make it difficult to detect the gradient. The SSDHR models also detect the decrease in slowness in the Holocene material beneath the compacted fill, as well as the decrease starting at about 63 m depth. In addition, the SSDHR models also capture some of the variations shown in the suspension log model between 15 and 63 m. Fig. 11 shows the amplifications that result from these models. The differences in amplifications are quite small for frequencies less than about 5 Hz, in spite of significant variation between the slowness models. We will see that it is true for most of the examples in this paper. This is an important observation, for it indicates that the fine layering in the models is not important for most earthquake engineering concerns

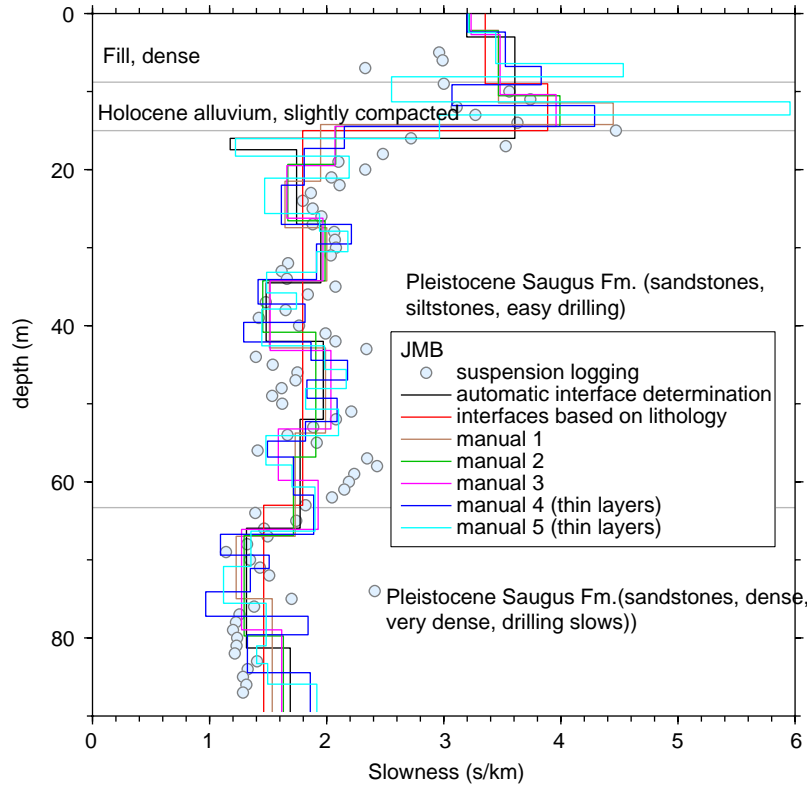


Fig. 10. Shear-wave slowness profiles at Jensen Main Building for slowness models derived using different sets of interface depths. “OFR 99-448” is the model of Ref. [20]. Also shown are slownesses from suspension-log measurements [33].

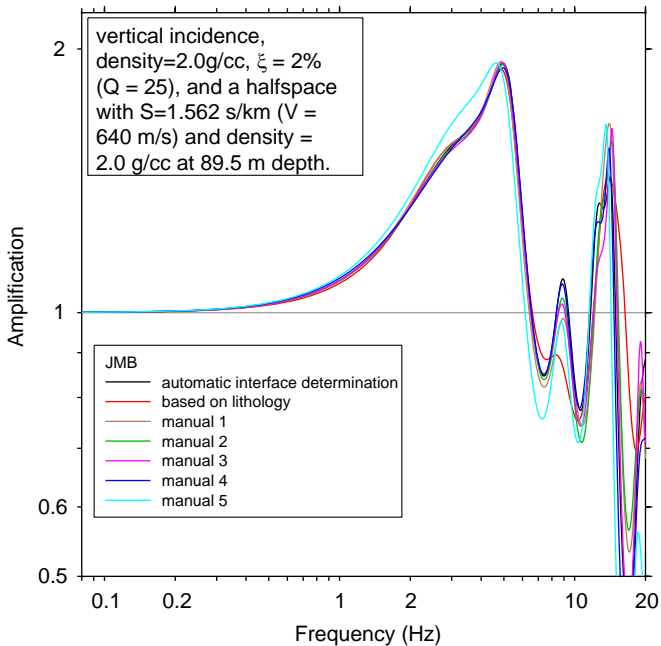


Fig. 11. Amplifications at Jensen Main Building for slowness models derived using different sets of interface depths. “OFR 99-448” is the model of Ref. [20]. Information about the amplifications, including the reference condition, is given in the figure.

(assuming that the ground motions of most importance to earthquake engineers are at frequencies less than about 5 Hz). Models made up of slowness averaged over 5 m or so

are often sufficient for estimating site amplification (we will see this in more detail in a later example).

4.2. A site with a large contrast in slowness (Grass)

The Grass site in Kyeongju, Korea studied by Kim et al. [11] is interesting for several reasons. First, the measured travel-time arrivals are more precise than those from most SSDHR surveys; second, the majority of the travel-time measurements are shallow, reaching a maximum depth of 16.1 m, relative to the horizontal offset of the source from the borehole of 3 m. Therefore, a significant amount of curvature in the travel-time data results from the ray-path. The most interesting aspect of this site, however, is a large decrease in slowness at a relatively shallow depth. The large contrast in slowness coupled with a horizontal offset of 3 m and the relatively shallow depths of the measurements causes the ray-path to diverge significantly from the straight line connecting the source to receiver. This causes the model produced by the inversion that accounts for refractions to be significantly different than the model produced by the inversion that does not account for refractions, at least in the vicinity of the interface. This also causes the travel-time data in this example to *decrease* with depth just below the interface.

The slowness plots for this site are shown in Fig. 12. The models include those computed with and without accounting for refractions at layer boundaries (for the same set of

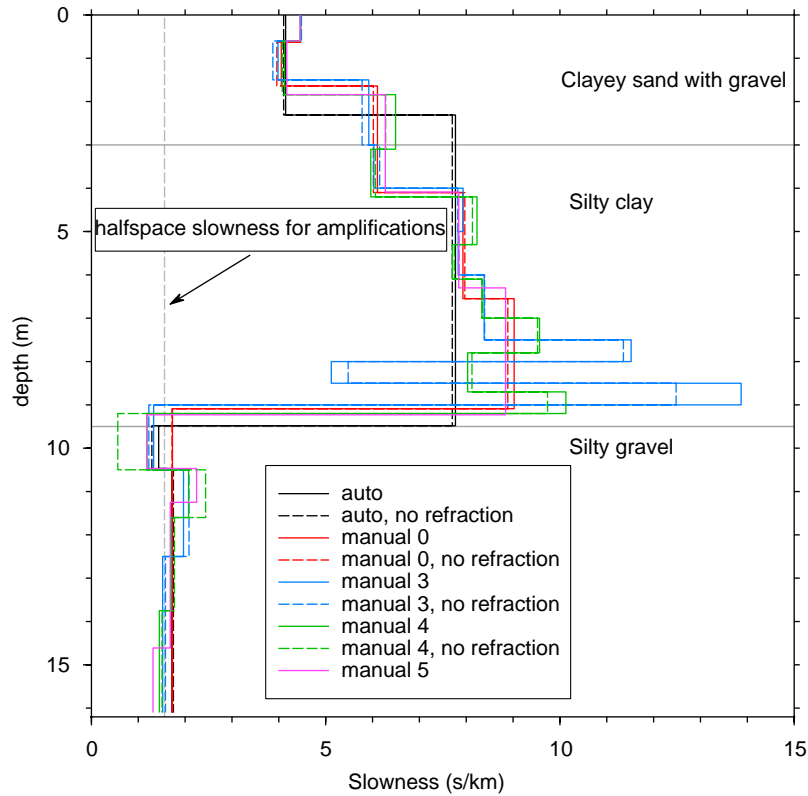


Fig. 12. Comparison of slowness profiles at Grass site, using travel-time data and lithologic descriptions from Kim et al. [11]. The “no refraction” models were derived using the same depths to interfaces as the model with the same name, but all ray-paths were assumed to be straight, with no correction for refractions at layer boundaries. The numbers following “manual” are arbitrary, and simply identify the model.

interface depths). As the figure shows, the difference between the models with and without refraction is small except near the large change in slowness at 9 m; the slownesses just below the interface differs by more than a factor of two. The model produced by the automatic determination of interface depths is particularly simple in this case, but it captures the essential features of the slowness profile. The amplifications are shown in Fig. 13. As for JMB, the amplifications are relatively insensitive to the details of the slowness model. Even the model produced by the routine for automatically finding layer interfaces results in amplifications that are surprisingly similar to those produced by the more detailed models. The peaks and troughs are in approximately the same locations; the peaks in amplification at approximately 3 and 10 Hz have nearly the same amplitudes in all the models, but the amplitude in the troughs at approximately 7 Hz has a significant amount of model-to-model variation (the largest deviation in amplitude is from the model with automatically picked interfaces).

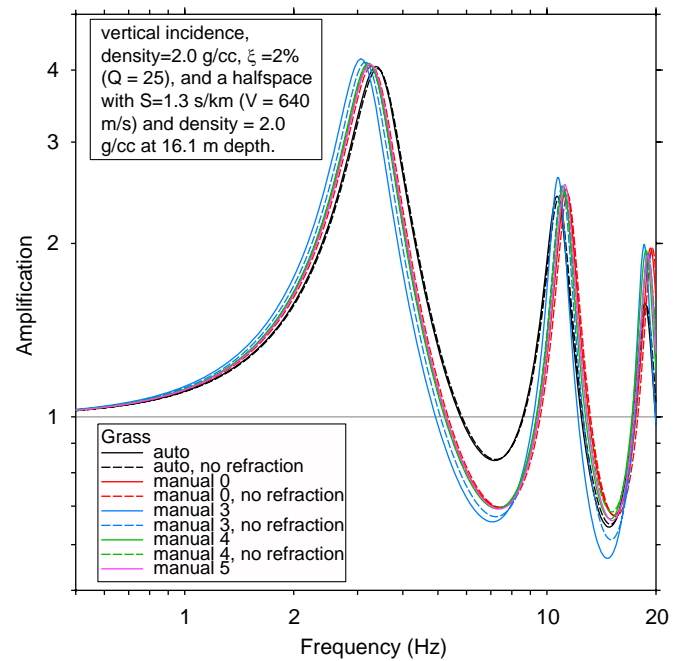


Fig. 13. Amplifications at GRASS for models shown in the previous figure. Information about the amplifications, including the reference condition, is given in the figure.

4.3. A site with a large variation in slowness over small depth ranges (WVAN)

The most difficult aspect of model selection is determining if fluctuations in the travel-time data indicate a layer interface or if they are produced by the scatter that results from the error in picking the travel-times. Thin layers, with

thicknesses comparable to or less than the sampling distance, are particularly difficult to identify because they will not be defined by a clear trend in the travel-time data.

A thin layer with contrasting slowness can sometimes be inferred even if no measurements have been made in the layer; a thin layer is likely present if the travel-time curve exhibits an offset that cannot be accounted for otherwise. To illustrate a case with many thin layers, we choose the Wadsworth VA Hospital, North (WVAN) site in Southern California [31]. This site is particularly interesting because the suspension-log data indicates significant variability in slowness, with several thin low-slowness layers. The site is also interesting because the uncertainties given by Gibbs et al. [31] are large at the deeper depths, as shown in Fig. 14, and thus the influence of the uncertainties on the derived model can be studied. Notice, however, that the travel-times for the most poorly determined arrivals show no more scatter than do the best determined values. This paradoxical observation is explained by the way in which the travel-times were picked by Gibbs et al. [31]: the arrival times were determined subjectively, with the arrivals at a given depth being influenced by the waveforms at nearby depths. This introduces an implicit correlation in the times at nearby depths. Fig. 15 compares several models with manually determined interfaces, the model with interfaces determined by the previously described automatic routine, and the suspension-log data. The travel-times for this site are somewhat uncertain at depth, and therefore one of the manual models made no attempt to reduce trends in the residuals at deeper depths. All models accurately model the strong decrease in slowness near the surface, and many of

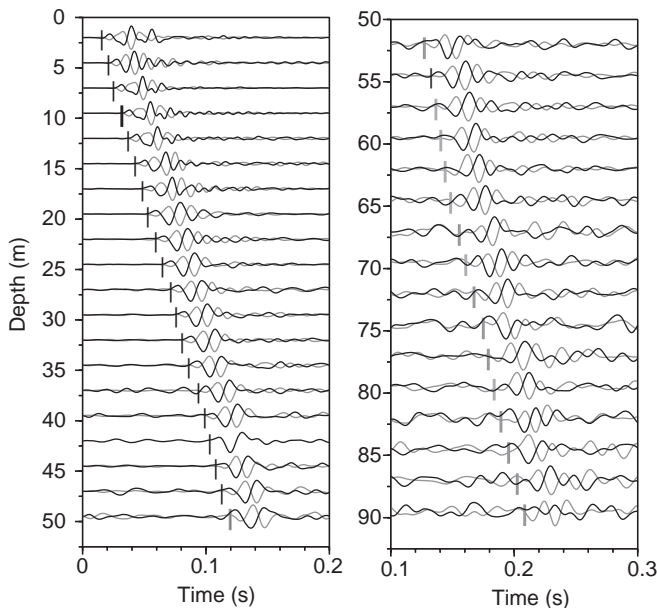


Fig. 14. Travel-time picks indicated by bars superimposed on the time series at the Wadsworth Veteran's Administration Hospital North site (WVAN) (adapted from Gibbs et al. [31]). The gray bars indicate travel-times that are less certain than the black bars (the darker and lighter shades of gray correspond to uncertainties twice and three to five times greater than the black bar, respectively). Note that the time scale for the right-hand panel of graphs starts at 0.1s, not 0.0s as in the left-hand panel.

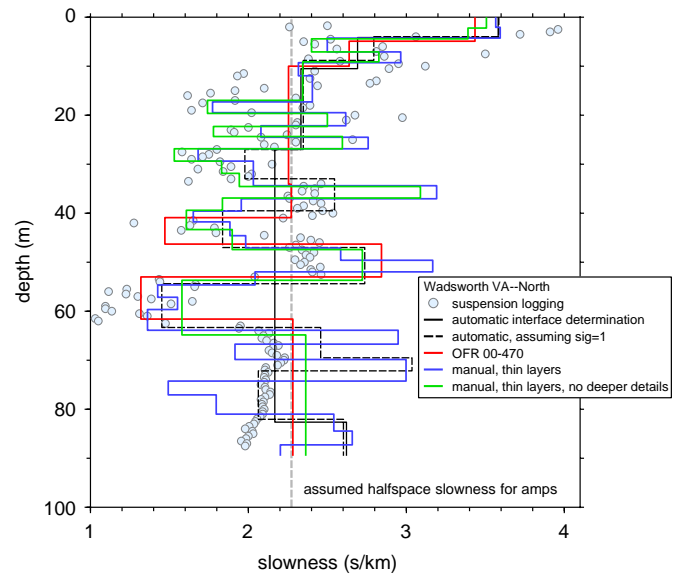


Fig. 15. Shear-wave slowness profiles at WVAN for slowness models derived using different sets of interface depths. “OFR 00-470” is the model of Gibbs et al. [31]. Also shown are slowness from suspension-log measurements [33]. To avoid increasing an already cluttered graph, the lithology is not shown. According to Figure A-55 in Gibbs et al. [31], the section consists of sands and silts to 41.5 m, sands and gravelly sands from 41.5 to 47 m, siltstone from 47 to 54 m, hard slate from 54 to 62 m, with the rest of the section consisting of siltstones and mudstones.

the detailed fluctuations in slowness indicated by the suspension-log data are also captured by the more detailed SSDHR models. Interestingly, the automatic picking routine finds only five layer interfaces at this site. The uncertainty of the picks at depth is reflected in the estimated variance ($\hat{\sigma}^2$), which causes the AIC_c to increase if more than five layers are added to the model. For comparison, we set all the relative estimates of the variance of each pick equal to one; in this case the automatic routine finds a twelve-layer model that eliminates all of the linear trends that are present in the residuals of the model with the initial automatically determined interfaces (when the relative estimates of travel-time variance are included). The thin layering in this twelve-layer model and the more complex manually picked model below approximately 65 m have large fluctuations, where the suspension-log data indicate that the slowness is remarkably constant across this interval.

As might be expected from the large variability in the slowness models, there is more variability in the amplifications (Fig. 16) than shown previously. But for frequencies less than about 5 Hz, the amplifications are quite similar, even for the simple model determined from the automatic algorithm.

4.4. A deep site with gradients and large variations in slowness over small depth ranges (I10)

Although the suspension-log data at both JMB and WVAN indicate that transition zones or slowness gradients

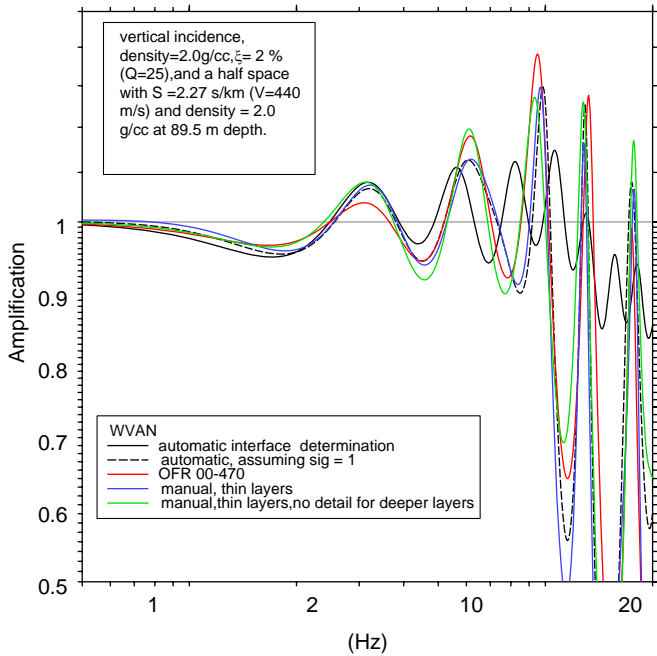


Fig. 16. Amplifications at WVAN for models shown in the previous figure. “OFR 00-470” is the model of Ref. [31]. Information about the amplifications, including the reference condition, is given in the figure. “sig = 1” means that the uncertainty in all travel-times was assumed to be the same.

may be present, the suspension-log data from the intersection of La Cienega Boulevard and Interstate 10 in southern California indicates a clear and sizable gradient in the shear-wave slowness of the near-surface sediments. See Boore et al. [32] for further details about this site. Fig. 17 compares multiple SSDHR slowness models with the suspension-log data, and the inset shows the details of the upper 75 m; Fig. 18 compares the corresponding amplifications that result from these models. The suspension-log data clearly indicate a gradual decrease in slowness from about 10 s/km at a depth of 2 m to approximately 3 s/km at 17 m. This provides an opportunity to determine the effect of approximating this transition zone with a stepwise function. All of the SSDHR models approximate this transition zone with three or four constant slowness layers. We vary the level of model detail, and include the automatically picked set of layer interfaces as in the other examples. This site also has the deepest data of all the examples, so the amplifications are valid at longer periods. The amplifications at this site show little variability at frequencies below 5 Hz.

5. Sensitivity of slowness and amplifications to layering

In addition to the previous comparisons of amplifications from various slowness models at a given site, in this section we study models of slowness at I10 made by averaging the suspension model over various depth ranges. Because the suspension log does not extend to the surface, we assumed a

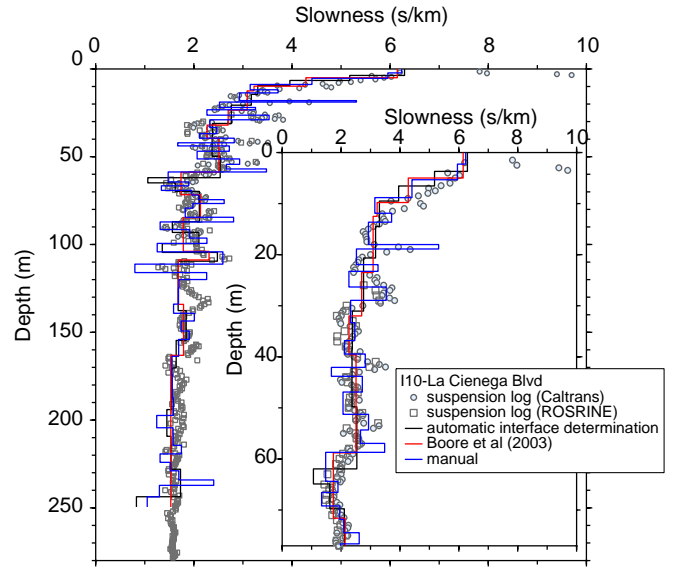


Fig. 17. Shear-wave slowness profiles at the I10—La Cienega Boulevard site for slowness models derived using different sets of interface depths and the surface-source downhole-receiver (SSDHR) arrival times. “Boore et al. (2003)” is the model of Ref. [32]. Also shown are slowness from suspension-log measurements [33] from the California Department of Transportation [34].

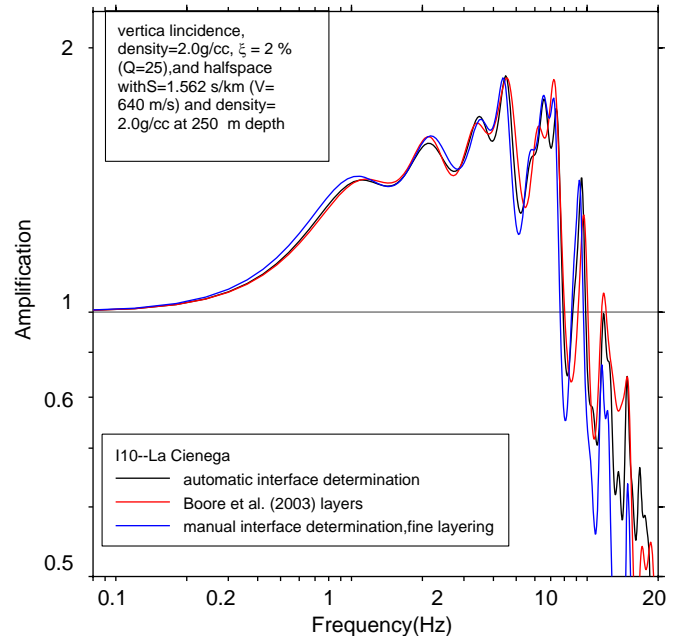


Fig. 18. Amplifications at the I10—La Cienega Boulevard site for models shown in the previous figure. “Boore et al. (2003)” is the model of Ref. [32]. Information about the amplifications, including the reference condition, is given in the figure.

representative value of slowness in the upper few meters. In all cases we constrain the average models to preserve the average of the suspension slowness over each depth interval. We use the suspension-log data for this section rather than SSDHR data because the sampling interval is finer and our

goal in this section is to demonstrate the sensitivity of site amplification to the details of layering rather than to study the inter-model variability that results from different interpretations of SSDHR surveys. Fig. 19 plots the slowness models averaged over intervals of 0.25, 0.50, 1.0, 2.5, 5.0, 7.5, and 10.0 m. The transition zone in the upper 20 m is only a few meters larger than the layer thickness in the model with the largest averaging interval. In contrast, the model with the smallest interval captures all of the detail of the suspension-log data because the averaging interval is equal to the sampling interval. The amplifications shown in Fig. 20, corresponding to the suite of slowness models in Fig. 19, indicate more model-to-model variability in amplitude above 2 Hz than the suite of SSDHR models compared in Fig. 17. This should be expected because the depth resolution of the suspension-log models is greater than for the SSDHR models. If we exclude the coarsest model (with 10.0 m averaging), then the amplifications are fairly similar at frequencies up to 5 Hz. If we also exclude the model with an averaging interval of 7.5 m, then differences in the amplifications are minor at frequencies up to 5 Hz.

6. Discussion and conclusions

We present a method for calculating a model of shear-wave slowness from SSDHR surveys. To analyze the uncertainty in the models, we use examples from several borehole surveys, each with multiple models fit to the observations (the method is equally applicable to measurements from SCPT surveys). Suspension log data provides

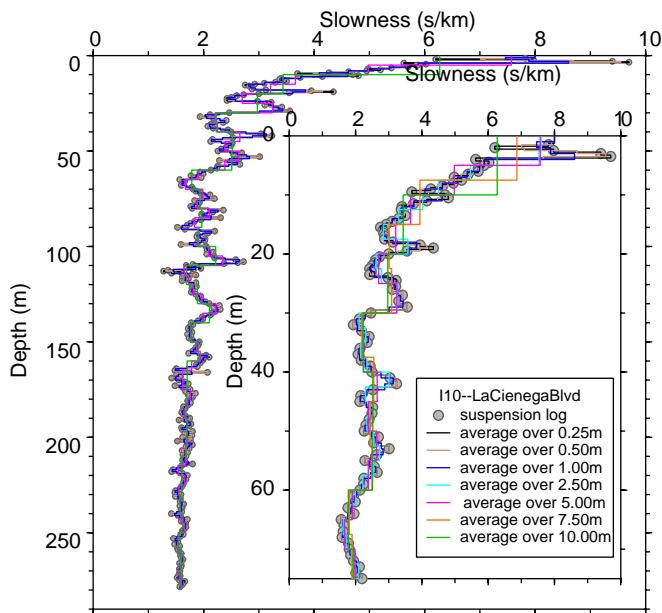


Fig. 19. Shear-wave slowness profiles at the I10—La Cienega Boulevard site based on averages over various depth intervals of the models based on suspension-logging measurements. The ROSRINE and Caltrans models have been merged to produce a single set of suspension-log values before averaging.

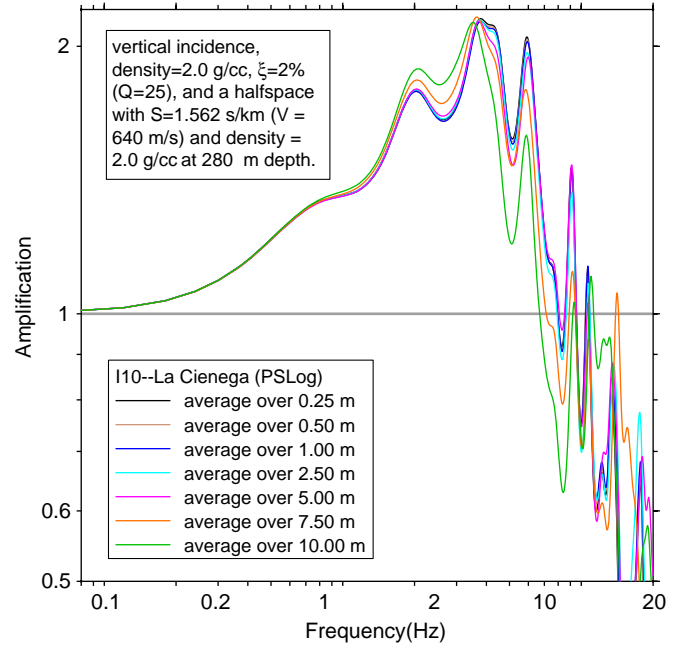


Fig. 20. Amplifications at the I10—La Cienega Boulevard site for models shown in the previous figure. Information about the amplifications, including the reference condition, is given in the figure.

an independent and more precise measurement of the slowness against which we can compare the models. By varying the number of parameters in the models and plotting the corresponding amplifications, we demonstrate that the amplifications below 5 Hz are relatively insensitive to the differences between models obtained by different interpretations. Although frequencies of concern to many earthquake engineers are lower than 5 Hz, there are a number of important applications for which higher frequencies are important (such as sensitive equipment, relays, piping systems, etc.). In such cases, differences in interpretation of slowness surveys can lead to significant differences in amplifications, and special care must be taken in such situations.

The location and number of interfaces that are indicated by the data at a particular site can be subjective, depending on the amount of layer-to-layer fluctuation in the seismic slowness that the analyst is willing to accept. We have found that some researchers have an aversion to large fluctuations and prefer models that closely adhere to the variations indicated by the geologic logs, whereas others are willing to accept rapid layer-to-layer fluctuations. While the comparison between grain-size changes and suspension logs by Wentworth and Tinsley [30] suggests that the real slowness can have rapid fluctuations, this level of precision is typically not resolved by SSDHR surveys (although this clearly depends on the sampling interval). Fortunately, site amplifications are little affected by fluctuations of slowness over depth intervals of a few meters. The subjectivity of interpretations is illustrated by the many examples that we have discussed in this paper.

One researcher may prefer the models strictly based on lithology, while another may prefer the more detailed models based on manually picked interfaces or even interval-slownesses.

The example at the WVAN site (Figs. 14 and 15) shows that the precision of the measured travel-times is an important factor to consider when choosing the number and location of the layer interfaces; if the uncertainty of the travel-time picks is large even clear linear trends in the data may be spurious. Comparing all the seismic traces from a borehole simultaneously will improve the accuracy with which the arrivals of seismic phases are identified. If the measurements were made “blind” with respect to the other traces, then the scatter in the picks would be larger and the resulting variance estimates of the slownesses would reflect the increased uncertainty in the picks.

In this paper we advocate a method of building slowness models iteratively by selecting interfaces based on patterns in the observed travel-time data. Model-selection uncertainty increases because data are used for both model selection (in our case, the depths to interfaces) and also to estimate the parameters of the model (the slowness of each layer and σ^2). Accounting for model-selection uncertainty is beyond the scope of this paper, but it should be noted that the estimates of variance provided in this paper (such as the plus and minus one standard deviation lines on slowness profiles) are probably too small because model-selection uncertainty is not included. This problem is magnified as the number of model parameters become large relative to the number of observations. The automatic routine we present uses AIC_c as an objective criterion for limiting the number of interfaces added to the model. In general, we have found that this results in a conservative estimate for the number of interfaces that are warranted by a SSDHR survey, and that most models can be improved by manually adjusting the layering. In many situations, however, the slowness models that result from the automatic routine may be preferred to interval-slownesses when the large fluctuations, typical of interval-slownesses, are not desired. The interval-slownesses are equivalent to our method when the location of layer interfaces are equal to the depth of each measurement, thus making the number of parameters in the inversion equal to the number of measurements. Interval-slownesses may do an adequate job when the errors in picking the travel-times are small, but can lead to complex slowness models that may or may not be a good representation of the true slowness beneath a site. This may be of little consequence for site-response analysis however, because the amplifications in the frequency range relevant for most engineering applications are not affected by these details.

Acknowledgments

Conversations with Robert Pyke and Kenneth Stokoe stimulated our thinking on transition regions of slowness. Mike Bennett and Rob Kayen provided useful reviews

of the manuscript. The participation of the second author is funded by National Science Foundation Grant CMS-0409311.

References

- [1] Dobry R, Borcherdt RD, Crouse CB, Idriss IM, Joyner WB, Martin GR, et al. New site coefficients and site classification system used in recent building seismic code provisions. *Earthquake Spectra* 2000; 16(1):41.
- [2] Somerville PG, Graves RW. Characterization of earthquake strong ground motion. *Pure Appl Geophys* 2003;160(10–11):1811.
- [3] Boore DM. Can site response be predicted? *J Earthquake Eng* 2004;81.
- [4] Boore DM. Determining subsurface shear-wave velocities: a review. In: Third international symposium on the effects of surface geology on seismic motion, Grenoble, France; 30 August–1 September 2006. Paper number: 103.
- [5] Boore DM. A compendium of P- and S-wave velocities from surface-to-borehole logging: summary and reanalysis of previously published data and analysis of unpublished data. U.S. Geol Surv Open-File Rept 03-191; 2003. 13pp.
- [6] Holzer TL, Bennett MJ, Noce TE, Tinsley III JC. Shear-wave velocity of surficial geologic sediments in Northern California: statistical distributions and depth dependence. *Earthquake Spectra* 2005;21(1):161.
- [7] Brocher TM. Empirical relations between elastic wavespeeds and density in the earth's crust. *Bull Seismol Soc Am* 2005;95(6):2081.
- [8] Brocher TM. A regional view of urban sedimentary basins in Northern California based on oil industry compressional-wave velocity and density logs. *Bull Seismol Soc Am* 2005;95(6):2093.
- [9] Andrus RD, Stokoe II KH. Liquefaction resistance of soils from shear-wave velocity. *J Geotech Geoenviron Eng* 2000;126(11):1015.
- [10] Kayen RE, Tanaka Y, Kishida T, Sugimoto S. Liquefaction potential of native ground in West Kobe, Japan by the Spectral Analysis of Surface Waves (SASW), method. 8th US–Japan workshop on earthquake-resistant design of lifeline facilities and counter measures against soil liquefaction, Tokyo, Japan, 16–18 December 2002.
- [11] Kim D, Bang E, Kim W. Evaluation of various downhole data reduction methods for obtaining reliable V_S profiles. *Geotech Test J* 2004;27(6):585.
- [12] Thompson EM. Downhole seismic analysis in R. U.S. Geol Surv Open-File Rept OF 2007-1124.
- [13] Brown LT, Boore DM, Stokoe II KH. Comparison of shear-wave slowness profiles at 10 strong-motion sites from noninvasive SASW measurements and measurements made in boreholes. *Bull Seismol Soc Am* 2002;92(8):3116.
- [14] Boore DM, Brown LT. Comparing shear-wave velocity profiles from inversion of surface-wave phase velocities with downhole measurements: systematic differences between the CXW method and downhole measurements at six USC strong-motion sites. *Seism Res Lett* 1998;69:222–9.
- [15] Boore DM, Brown LT. Erratum: comparing shear-wave velocity profiles from inversion of surface-wave phase velocities with downhole measurements: systematic differences between the CXW method and downhole measurements at six USC strong-motion sites. Correction of Fig. 5. *Seism Res Lett* 1998;69:406.
- [16] Karl L, Haegeman W, Degrande G. Determination of the material damping ratio and the shear wave velocity with the seismic cone penetration test. *Soil Dyn Earthquake Eng* 2006;26(12):1111.
- [17] Liu H, Hu Y, Dorman J, Chang T, Chiu J. Upper Mississippi embayment shallow seismic velocities measured in situ. *Eng Geol* 1997;46(3–4):313.
- [18] Mok YJ. Analytical and experimental studies of borehole seismic methods. Ph.D. Thesis, University of Texas, 1987. 272pp.

- [19] R Development Core Team. R: a language and environment for statistical computing. R Foundation for Statistical Computing, Vienna, Austria; 2006.
- [20] Gibbs JF, Tinsley III JC, Boore DM, Joyner WB. Seismic velocities and geological conditions at twelve sites subjected to strong ground motion in the 1994 Northridge, California, earthquake: a revision of OFR 96-740. U.S. Geol Surv Open-File Rept 99-446; 1999. 142pp.
- [21] Akaike H. New look at the statistical model identification. *IEEE Trans Autom Control* 1974;AC-19(6):716.
- [22] Sugiura N. Further analysis of data by Akaike's information criterion and finite corrections. *Commun Stat Part A—Theory Methods* 1978;7(1):13.
- [23] Burnham KP, Anderson DR. Model selection and multimodel inference: a practical information-theoretic approach. New York: Springer; 2002.
- [24] Mueller C. Written communication; 1984.
- [25] Herrmann R. Written communication; 1998.
- [26] Boore DM. SMSIM—Fortran programs for simulating ground motions from earthquakes: version 2.3. A Revision of U.S. Geol Surv Open-File-Report 96-80-A; 2005. 55pp.
- [27] Nigbor RL, Imai T. The suspension P-S velocity logging method, geophysical characterization of sites, ISSMFE special publication TC 10; 1994.
- [28] Diehl JG, Martin AJ, Steller RA. Twenty year retrospective on the Oyo P-S suspension logger. In: Proceedings of the 8th US national conference on earthquake engineering, San Francisco, CA, 18–22 April 2006. DRC/SSA/EERI.
- [29] GEOVision Inc. Suspension P-S Velocity Logging Method. 2006(10/24): <http://www.geovision.com/PDF/M_PS_Logging.PDF>.
- [30] Wentworth CM, Tinsley III JC. Geologic setting, stratigraphy, and detailed velocity structure of the Coyote Creek borehole, Santa Clara Valley, California. In: Asten, MW, Boore, DM, editors. Blind comparisons of shear-wave velocities at closely-spaced sites in San Jose, California. U.S. Geol Surv Open-File Rept 05-1169, part 2; 2005. 26pp.
- [31] Gibbs JF, Tinsley III JC, Boore DM, Joyner WB. Borehole velocity measurements and geological conditions at thirteen sites in the Los Angeles, California region. U.S. Geol Surv Open-File Rept 00-470; 2000. 118pp.
- [32] Boore DM, Gibbs JF, Joyner WB, Tinsley III JC, Ponti DJ. Estimated ground motion from the 1994 Northridge, California, earthquake at the site of interstate 10 and La Cienega Boulevard bridge collapse, West Los Angeles, CA. *Bull Seismol Soc Am* 2003;93(6):2737.
- [33] ROSRINE. Resolution of site response issues from the Northridge Earthquake. 2006(10/24): <<http://geoinfo.usc.edu/rosrine/>>.
- [34] Roblee C. Written communication; 1999.